Self-interaction correction for density-functional theory of electronic energy bands of solids

Richard A. Heaton, Joseph G. Harrison,* and Chun C. Lin

Department of Physics, University of Wisconsin, Madison, Wisconsin 53706

(Received 23 March 1983)

Although the self-interaction terms in the Coulomb and exchange potentials exactly cancel each other in the Hartree-Fock one-electron Hamiltonian, the cancellation is incomplete when the exchange interaction is treated by the density-functional approximation. The residual self-interaction pushes the orbital energy levels upward. This effect is especially serious for valence states of insulators with localized charge distribution and causes an underestimation of the energy band gap. We have corrected for this incomplete cancellation of self-interaction in the density-functional formalism of energy-band theory of crystalline solids. The self-interaction correction (SIC) to the total energy of the N-electron system is expressed in terms of the Wannier functions, and periodic SIC potentials for the Bloch-state wave functions are derived variationally from the energy functional. The resulting SIC one-electron Hamiltonians are state dependent, but a unified Hamiltonian has been devised so that energies of all levels of the same $\vec{k}$ from different bands are obtained by diagonalizing the same matrix. We have applied this SIC method to calculate the energy band structure of the argon and LiCl crystals. Using the Kohn-Sham exchange along with the correlation potential of von Barth and Hedin, we obtain band gaps in excellent agreement with experiment, whereas without SIC the calculated band gaps are more than 35% below the experimental values.

I. INTRODUCTION

In the Hartree-Fock (HF) theory of many-electron systems, an individual one-electron orbital is governed by the interaction of that electron with the nuclei and with all other electrons. The latter is usually divided into a Coulomb potential and an exchange potential. It is customary to include in both the Coulomb and exchange potentials a term corresponding to the interaction of the electron with itself.[1] Since the self-Coulomb and self-exchange interaction exactly cancel each other, inclusion of these physically unrealistic terms does not alter the self-consistent-field (SCF) equations, but has the advantage of making the Coulomb potential and exchange potential reflect separately the symmetry of the system. However, when the exchange potential is treated by the local-density-functional (LDF) approximation,[2] the cancellation of the self-interaction terms is no longer exact. A consequence of this deficiency is that the atomic energy levels (relative to the ionization limit) calculated by the LDF approximation are too high. The problem of this incomplete cancellation of self-interaction has long been recognized and methods for correcting it have been suggested in numerous papers.[3-11] Of the more recent works our attention is drawn particularly to the formulation of self-interaction correction (SIC) by Lindgren[4] and by Perdew[5] which have been applied to atoms (including negative ions) very successfully.

For SCF energy-band calculations of crystals, it is known that application of the LDF theory to ionic crystals leads to a band gap typically 40% below the experimental value.[6,12,13] This discrepancy can be attributed, at least partially, to the residual self-interaction which tends to push the energy levels upward. The valence states have

a more localized charge distribution than do the conduction states and thus a larger self-interaction error, resulting in a smaller band gap. However, incorporation of SIC into the SCF equations for the Bloch-type wave functions of crystals is much more difficult than the case of free atoms, and relatively few papers dealing with the SIC for crystal band-structure calculations have appeared in the literature.[6,9-11]

In Ref. 14 we presented a brief outline of a formulation of the SIC for the energy-band theory of crystals with application to the specific case of LiCl. Our treatment differs from the ones cited above in that we derive a periodic SIC potential for the Bloch-type wave functions variationally in the LDF framework rather than focusing primarily on the SIC for localized orbitals in the solid. In the present paper a full account of the theoretical foundation of our treatment of the SIC is given, and applications to the LiCl and Ar crystals are made. Computational techniques for handling the SIC terms are also prescribed. In Sec. IV an approximation appropriate to large-gap insulators is introduced so that the inclusion of SIC entails only a minor increase of the computational work in the band-structure calculation.

II. PRELIMINARY CONSIDERATION

Let us denote an orbital electron density by $\rho_{i\sigma}(\vec{r})$ with σ being the spin index ($\uparrow$ or $\downarrow$), the total electron density by $\rho(\vec{r})$, and the spin density by $\rho_\sigma(\vec{r})$. Following Perdew's work[5] we write the energy functional as the sum of the kinetic energy, external interaction, Coulomb energy, exchange correlation, and the SIC term,

$$E_t = T + V_{\text{ext}} + U_C + E_{\text{xc}} + U_{\text{SIC}} , \tag{1}$$

$$U_C[\rho] = \tfrac{1}{2} \int \rho(\vec{r})\rho(\vec{r}') \,|\, \vec{r} - \vec{r}' \,|^{-1} d\vec{r} \, d\vec{r}' , \tag{2}$$

$$E_{\text{xc}}(\rho_\uparrow, \rho_\downarrow) = \int \rho(\vec{r})\epsilon_{\text{xc}}[\rho_\uparrow, \rho_\downarrow] d\vec{r} , \tag{3}$$

$$U_{\text{SIC}} = -\sum_{i,\sigma} (U_C[\rho_{i\sigma}] + E_{\text{xc}}[\rho_{i\sigma}, 0]) , \tag{4}$$

where $\epsilon_{\text{xc}}[\rho_\uparrow, \rho_\downarrow]$ is the exchange-correlation energy of an electron gas with uniform spin densities $\rho_\uparrow$ and $\rho_\downarrow$. The SCF equations for the electron orbitals are then derived from the energy functional. The one-electron Hamiltonian is found to have the form

$$H_{i\sigma} = -\tfrac{1}{2}\nabla^2 + V_0 + V_{i\sigma}^{\text{SIC}} , \tag{5}$$

in which V_0 is the sum of the electron-nucleus, electron-electron, and exchange-correlation potentials as in the local-spin-density (LSD) theory, and

$$V_{i\sigma}^{\text{SIC}}(\vec{r}) = -\int \frac{\rho_{i\sigma}(\vec{r}')}{|\vec{r} - \vec{r}'|} d\vec{r}'$$
$$- \frac{\partial}{\partial \rho_{i\sigma}} \{\rho_{i\sigma}(\vec{r})\epsilon_{\text{xc}}[\rho_{i\sigma}, 0]\} . \tag{6}$$

With the exchange-only formula of Kohn and Sham,[2] Eq. (6) reduces to

$$V_{i\sigma}^{\text{SIC}}(\vec{r}) = -\int \rho_{i\sigma}(\vec{r}') \,|\, \vec{r} - \vec{r}' \,|^{-1} d\vec{r}' + [(6/\pi)\rho_{i\sigma}(\vec{r})]^{1/3} . \tag{7}$$

The SIC potential for free atoms can be readily evaluated from Eq. (6) and inclusion of this term leads to a remarkable improvement of the energy levels.[4-7] For electrons in a crystal, the wave functions are normally written in the form of a Bloch wave which extends over the entire crystal. Such a completely delocalized electron density gives zero V^{SIC} from Eq. (6). This may seem to suggest that no SIC is needed for solids. However, for crystals with no incompletely filled bands, it is possible to express the electronic wave function in the localized Wannier form. When the orbital density is taken as the absolute square of the Wannier function, the SIC is clearly not equal to zero. Thus the magnitude of the SIC term depends on the choice of representation. The question then arises as to which representation is the appropriate one for SIC. To address this point let us consider a simple example as follows. Imagine two atoms separated by a large distance R. Each atom has one electron, and for this analysis no reference to electron spin will be made explicitly. We denote the two atoms by A and B and the two electrons by 1 and 2. In a localized representation the one-electron orbitals are simply the free-atom wave function, $w_A(\vec{r}_1)$ and $w_B(\vec{r}_2)$, where the subscript A refers to the wave function of an electron at atom A. The Coulomb energy U_C is calculated by using Eq. (2) with

$$\rho(\vec{r}) = |\, w_A(\vec{r}) \,|^2 + |\, w_B(\vec{r}) \,|^2 . \tag{8}$$

Dividing the Coulomb energy into a self-interaction term and an interelectron term as

$$U_C = U_C^S + U_C^I , \tag{9}$$

we have, from Eqs. (2) and (8),

$$U_C^S = \int |\, w_A(\vec{r}) \,|^2 |\, w_A(\vec{r}') \,|^2 |\, \vec{r} - \vec{r}' \,|^{-1} d\vec{r} \, d\vec{r}' , \tag{10}$$

$$U_C^I = \int |\, w_A(\vec{r}) \,|^2 |\, w_B(\vec{r}') \,|^2 |\, \vec{r} - \vec{r}' \,|^{-1} d\vec{r} \, d\vec{r}' . \tag{11}$$

For large R, U_C^I is much smaller than U_C^S. A similar partition is introduced for the exchange energy so that

$$U_X = -\frac{1}{2} \sum_{i,j=A}^{B} \int w_i(\vec{r})w_j(\vec{r}') \,|\, \vec{r} - \vec{r}' \,|^{-1}$$
$$\times w_i(\vec{r}')w_j(\vec{r}) d\vec{r} \, d\vec{r}' = U_X^S + U_X^I , \tag{12}$$

$$U_X^S = -\int |\, w_A(\vec{r}) \,|^2 |\, w_A(\vec{r}') \,|^2 |\, \vec{r} - \vec{r}' \,|^{-1} d\vec{r} \, d\vec{r}' , \tag{13}$$

$$U_X^I = -\int w_A(\vec{r})w_B(\vec{r}') \,|\, \vec{r} - \vec{r}' \,|^{-1} w_A(\vec{r}')w_B(\vec{r}) d\vec{r} \, d\vec{r}' . \tag{14}$$

We see that U_X^S is just the negative of U_C^S. In the HF method these two terms cancel each other and the interelectron terms are small at large R so that the total $U_C + U_X$ is small. When the standard local-density approximation (LDA) is applied to the full U_X, the incomplete cancellation of the self-interaction may result in a gross overestimation of the absolute magnitude of $U_C + U_X$. With SIC the large self-interaction is removed at the outset and only the small interelectron exchange is treated by approximation. One can then expect good accuracy by the SIC-LSD approximation.

Let us now turn to the delocalized molecular-orbital representation where the wave functions for the two electrons are

$$\phi_\pm(\vec{r}) = [w_A(\vec{r}) \pm w_B(\vec{r})]/\sqrt{2} . \tag{15}$$

We recalculate the Coulomb and exchange energies in this representation, designated as W_C and W_X. Their self-interaction and interelectron components are W_C^S, W_X^S, W_C^I, and W_X^I. It is easily shown that

$$W_C^S = \tfrac{1}{2} \sum_{i=+,-} \int |\, \phi_i(\vec{r}) \,|^2 |\, \phi_i(\vec{r}') \,|^2 |\, \vec{r} - \vec{r}' \,|^{-1} d\vec{r} \, d\vec{r}'$$
$$\simeq \tfrac{1}{2} U_C^S , \tag{16}$$

where the "approximately equals" sign applies for the case of large R. The self-interaction Coulomb energy in the delocalized representation amounts to only one-half of the corresponding term in the localized representation. The other half of U_C^S turns into a mutual interaction in the delocalized representation as

$$W_C^I = \int |\, \phi_+(\vec{r}) \,|^2 |\, \phi_-(\vec{r}') \,|^2 |\, \vec{r} - \vec{r}' \,|^{-1} d\vec{r} \, d\vec{r}' \simeq \tfrac{1}{2} U_C^S . \tag{17}$$

Similarly we find

$$W_X^S = -W_C^S \simeq \tfrac{1}{2} U_X^S , \tag{18}$$

$$W_X^I \simeq \tfrac{1}{2} U_X^S . \tag{19}$$

In going from the localized to the delocalized representation we transfer half of the self-interaction into mutual interaction. Application of the SIC in the delocalized representation removes only the W^S terms, i.e., only half of the "true" self-interaction. Moreover, W_C^I and W_X^I (much larger than U_C^I and U_X^I) should almost cancel each other completely in the HF theory, but with the LSD approximation for W_X^I the incomplete cancellation may result in a serious error.

The above example shows that the self-interaction energy may partially transfer into mutual-interaction energy upon changing from one representation to another so that the distinction between self-interaction and mutual interaction is not always clearcut. One can, of course, apply the SIC using any representation to seek an improvement over the uncorrected LSD work. However, in some representations, such as the molecular-orbital representation referred to earlier, the SIC is not completely effective. This occurs when the inter-Coulomb and the interexchange terms should largely cancel each other but the use of the density-functional approximation spoils this cancellation. The SIC works better in a representation where the interelectron exchange is small and self-interaction is large. The magnitude of the self-energy is closely related to the concept of localized orbitals and is sometimes taken as a quantitative measure of the degree of localization of the orbitals.[15] In the case of crystalline solids when the orbitals are written in the Bloch form, the self-interaction disappears as it is entirely transformed into interelectron terms. Application of the SIC, therefore, must be made in a localized representation in order to realistically remove the self-interaction energy.

III. FORMULATION

A. Simple bands and composite bands

In the standard LSD theory the non-SIC Hamiltonian (with spin-polarization option) for a monatomic crystal is

$$H_{0\sigma} = -\tfrac{1}{2}\nabla^2 - \sum_\nu Z\,|\vec{r}-\vec{R}_\nu|^{-1}$$

$$+ \int \rho(\vec{r}')\,|\vec{r}-\vec{r}'|^{-1}d\vec{r}' + V_{xc,\sigma}[\rho_\uparrow,\rho_\downarrow] , \quad (20)$$

where $\vec{R}_\nu$ refers to a lattice site and the last term is the exchange-correlation potential. Incorporation of the SIC into the LSD theory for solids, as we have seen in the last section, requires realistic local orbital densities. In this paper we shall not attempt a systematic search for the optimal choice of the local orbitals (see discussion in Sec. VI). For the purpose of this work it is sufficient to demand that any orbital basis employed to define the SIC potential must be localized, be obtainable from a variation of the total-energy functional, and possess enough variational freedom to modify its localization in accordance with the variation of total energy. These criteria are satisfied by the Wannier functions (WF's) which have the following favorable characteristics. (1) WF's are related to the Bloch-state functions through a simple transformation, (2) WF's reduce to atomic orbitals in the tight-binding limit of deep core states, (3) WF's conform to the

bonding nature of the atoms in the crystal, and (4) WF's are at least exponentially localized for a proper and fixed choice of phase for the Bloch-state functions, e.g., for simple bands $\psi_{\vec{k}}(r=0)$ being real and positive.[16]

We shall consider first the case of a monatomic crystal with only simple bands. Furthermore, we confine our attention to crystals where all bands are either completely filled or empty. To construct the SIC part of the energy functional, we write the orbital density in the Wannier form

$$\rho_{i\sigma}(\vec{r}) = \rho_{n\sigma}(\vec{r}-\vec{R}_\nu) = |\,w_{n\sigma}(\vec{r}-\vec{R}_\nu)\,|^2 , \quad (21)$$

where $w_{n\sigma}(\vec{r}-\vec{R}_\nu)$ is the WF at the $\vec{R}_\nu$ site, and n is the band index. Equation (4) then leads to

$$U_{\text{SIC}} = -\sum_{n\sigma\nu}\{\,U_C[\rho_{n\sigma}(\vec{r}-\vec{R}_\nu)]$$

$$+E_{\text{xc}}[\rho_{n\sigma}(\vec{r}-\vec{R}_\nu),0]\} . \quad (22)$$

Upon expressing the total-energy functional in terms of the WF at all sites and minimizing the former with respect to the latter, we obtain an effective site-dependent one-electron Hamiltonian,

$$H_{n\sigma\nu} = H_0 + V_{n\sigma}^{\text{SIC}}(\vec{r}-\vec{R}_\nu) , \quad (23)$$

$$V_{n\sigma}^{\text{SIC}}(\vec{r}-\vec{R}_\nu) = -\int \rho_{n\sigma}(\vec{r}'-\vec{R}_\nu)\,|\,\vec{r}-\vec{r}'\,|^{-1}d\vec{r}'$$

$$+ V_{xc,\sigma}[\rho_{n\sigma}(\vec{r}-\vec{R}_\nu),0] , \quad (24)$$

and a set of SCF Schrödinger equations for the WF,

$$H_{n\sigma\nu}w_{n\sigma}(\vec{r}-\vec{R}_\nu) = \sum_{n',\xi}\epsilon_{n'\xi,n\nu}w_{n'\sigma}(\vec{r}-\vec{R}_\xi) , \quad (25)$$

where $\epsilon_{n'\xi,n\nu}$ is a Lagrange multiplier. We delete the σ index in H_0 since it is not needed for fully occupied bands.

The effective SIC potential $(V_{n\sigma}^{\text{SIC}})$ for the WF has essentially the same form as the atomic SIC potential if we compare Eqs. (24) and (20) with Eq. (7). In fact, it is interesting to note that $H_{n\sigma\nu}$ in Eq. (23) is the intuitive form one might choose upon naively placing the atomic system in a periodic crystal field. Another interesting feature of Eqs. (23)–(25) is the site dependence of the Hamiltonian; given the periodic form of U_{SIC} required by the periodic crystal symmetry, it is not entirely clear why the SIC potential should possess a site dependence and whether that site dependence "breaks" the crystal periodicity. However, one notes that the solution $w_{n\sigma}(\vec{r}-\vec{R}_\nu)$ is the same for all $\vec{R}_\nu$ sites, thus the periodicity of the charge density is ensured. The periodicity of the SIC Hamiltonian can be brought out more directly upon expressing the WF in terms of the Bloch waves through

$$\psi_{n\sigma\vec{k}}(\vec{r}) = N^{-1/2}\sum_\nu e^{i\vec{k}\cdot\vec{R}_\nu}w_{n\sigma}(\vec{r}-\vec{R}_\nu) . \quad (26)$$

Equations (23)–(25) are converted into a set of SCF equations for the Bloch-state wave functions with a $\vec{k}$-dependent, one-electron Hamiltonian (see Appendix A),

$$H_{n\sigma\vec{k}} = H_0 + \Delta V^{\text{SIC}}_{n\sigma\vec{k}}(\vec{r}) \, , \tag{27}$$

$$\Delta V^{\text{SIC}}_{n\sigma\vec{k}} = \sum_\nu \Theta_{n\sigma\vec{k}}(\vec{r}-\vec{R}_\nu) V^{\text{SIC}}_{n\sigma}(\vec{r}-\vec{R}_\nu) \, , \tag{28}$$

$$\Theta_{n\sigma\vec{k}}(\vec{r}-\vec{R}_\nu) = N^{-1/2} e^{i\vec{k}\cdot\vec{R}_\nu} w_{n\sigma}(\vec{r}-\vec{R}_\nu)/\psi_{n\sigma\vec{k}}(\vec{r}) \, , \tag{29}$$

$$H_{n\sigma\vec{k}}\psi_{n\sigma\vec{k}}(\vec{r}) = \sum_{n'} \epsilon_{n'\vec{k},n\vec{k}} \psi_{n'\sigma\vec{k}}(\vec{r}) \, , \tag{30}$$

where $\epsilon_{n'\vec{k},n\vec{k}}$ is a Lagrange multiplier. The nondiagonal multipliers cannot be eliminated by the usual transformation since the energy functional depends on the individual orbital densities. Equations (27)–(30) can also be derived by expressing U_{SIC} in terms of the Bloch-state wave functions and varying E_t with respect to all the $\psi_{n\sigma\vec{k}}$'s. We use the symbol ΔV^{SIC} to designate the SIC potential for the Bloch states in order to distinguish it from V^{SIC} which is the SIC potential for the localized orbitals. It is easy to show that ΔV^{SIC} is periodic, thus the space-group symmetry of the crystal is not broken. Apparently the SIC potential for the Bloch states is a lattice summation of the SIC potential for the localized orbitals multiplied by a modulating prefactor $\Theta_{n\sigma\vec{k}}(\vec{r}-\vec{R}_\nu)$. The effect of this prefactor can be understood by realizing that it possesses the property

$$\sum_\nu \Theta_{n\sigma\vec{k}}(\vec{r}-\vec{R}_\nu) = 1 \, . \tag{31}$$

This interesting result suggests a simple interpretation of $\Theta_{n\sigma\vec{k}}$. If we regard $\psi_{n\sigma\vec{k}}$ as a delocalized state having a weighting factor corresponding to the probability of originating from each site, then at some point r_0, $\Theta_{n\sigma\vec{k}}(\vec{r}_0-\vec{R}_\nu)$ is the weighting factor of $\psi_{n\sigma\vec{k}}$ being associated with site $\vec{R}_\nu$. The validity of this model becomes self-evident for a deep core state. Here the Bloch wave function is delocalized, yet a deep core state intuitively cannot be expected to differ substantially from the free-ion solution in terms of ionization energies and local-orbital charge density (aside from a Madelung-type shift). Thus the delocalization of the Bloch wave function in this case results from the probability of originating from different sites and does not represent a true spreading of the charge density around each site. The factor $\Theta_{n\sigma\vec{k}}$ ensures that the self-interaction energy corresponds to that of only one electron. As a further demonstration of the relation between the two forms of SIC potentials we take the SIC energy for each Bloch state, sum it over the entire band, and divide by the number of atoms, i.e.,

$$N^{-1} \sum_{\vec{k}} \langle \psi_{n\sigma\vec{k}} | \Delta V^{\text{SIC}}_{n\sigma\vec{k}}(\vec{r}) | \psi_{n\sigma\vec{k}} \rangle \, . \tag{32}$$

This should be equivalent to the average SIC energy per atom. Substitution of Eqs. (26), (28), and (29) reduces the above expression into

$$N^{-2} \sum_{\vec{k},\mu,\nu} \int e^{i\vec{k}\cdot(\vec{R}_\nu-\vec{R}_\mu)} w^*_{n\sigma}(\vec{r}-\vec{R}_\mu) w_{n\sigma}(\vec{r}-\vec{R}_\nu) V^{\text{SIC}}_{n\sigma}(\vec{r}-\vec{R}_\nu) d\vec{r}$$

$$= N^{-1} \sum_{\mu,\nu} \delta_{\mu,\nu} \int w^*_{n\sigma}(\vec{r}-\vec{R}_\mu) V^{\text{SIC}}_{n\sigma}(\vec{r}-\vec{R}_\nu) w_{n\sigma}(\vec{r}-\vec{R}_\nu) d\vec{r}$$

$$= \int w^*_{n\sigma}(\vec{r}-\vec{R}_\nu) V^{\text{SIC}}_{n\sigma}(\vec{r}-\vec{R}_\nu) w_{n\sigma}(\vec{r}-\vec{R}_\nu) d\vec{r} \, , \tag{33}$$

which is just the SIC energy for each site in the Wannier representation.

The two versions of SIC one-electron Hamiltonian for the Bloch states and for the WF's, as given in Eqs. (23) and (27), may be brought to a common form by introducing the projection operator $P_{n\sigma\nu}$,

$$P_{n\sigma\nu} f(\vec{r}) = \langle w_{n\sigma}(\vec{r}-\vec{R}_\nu) | f(\vec{r}) \rangle w_{n\sigma}(\vec{r}-\vec{R}_\nu) \, , \tag{34}$$

and defining

$$\bar{H} \equiv H_0 + \sum_{\mu,n} V^{\text{SIC}}_{n\sigma}(\vec{r}-\vec{R}_\mu) P_{n\sigma\mu} \, . \tag{35}$$

Because of the site orthogonality of the Wannier functions, we have

$$\bar{H} w_{n\sigma}(\vec{r}-\vec{R}_\nu) = [H_0 + V^{\text{SIC}}_{n\sigma}(\vec{r}-\vec{R}_\nu)] w_{n\sigma}(\vec{r}-\vec{R}_\nu) \, , \tag{36}$$

so that $\bar{H}$ may be regarded as a common Hamiltonian for the WF at all sites. Unlike the Hamiltonian $H_{n\sigma\nu}$ for the individual WF [Eq. (23)], $\bar{H}$ exhibits the periodicity of the crystal. Let us now operate $\bar{H}$ on a Bloch wave function,

$$\bar{H}\psi_{n\sigma\vec{k}} = H_0\psi_{n\sigma\vec{k}} + \sum_\nu V^{\text{SIC}}_{n\sigma}(\vec{r}-\vec{R}_\nu)\langle w_{n\sigma}(\vec{r}-\vec{R}_\nu) | \psi_{n\sigma\vec{k}} \rangle w_{n\sigma}(\vec{r}-\vec{R}_\nu)$$

$$= \left[H_0 + \sum_\nu V^{\text{SIC}}_{n\sigma}(\vec{r}-\vec{R}_\nu) N^{-1/2} e^{i\vec{k}\cdot\vec{R}_\nu} w_{n\sigma}(\vec{r}-\vec{R}_\nu)/\psi_{n\sigma\vec{k}} \right] \psi_{n\sigma\vec{k}} = [H_0 + \Delta V^{\text{SIC}}_{n\sigma\vec{k}}(\vec{r})]\psi_{n\sigma\vec{k}} \, . \tag{37}$$

Thus the common $\overline{H}$ operator applies to the WF's for all sites as well as the Bloch wave functions.

Since the Bloch functions are more convenient for actual computation, we shall seek a solution using the Bloch form and compute the necessary WF's directly from that solution. In Sec. IV we introduce approximate forms of the WF's which are less taxing to compute.

For composite bands the general approach is to transform the occupied subbands (index s) at a $\vec{k}$ point into a set of symmetrized subbands, labeled by local symmetry index m, which can be individually summed over the Brillouin zone (BZ) to generate the WF,[16] i.e.,

$$w_{nm\sigma}(\vec{r}-\vec{R}_v)=N^{-1/2}\sum_{\vec{k}}e^{-i\vec{k}\cdot\vec{R}_v}\left[\sum_s U_{sm}(\vec{k})\psi_{ns\sigma\vec{k}}(\vec{r})\right].$$

(38)

The symmetry constraints which specify both the irreducible representation for which $w_{nm\sigma}$ is a partner and the local bonding sites, $\vec{R}_v$, have been established elsewhere.[17] In contrast to the simple-band case described previously, in general, the $w_{nm\sigma}$'s are not spherical but conform to the local bonding character. The SIC functional still has the form of Eq. (22) provided we replace the local-orbital density $\rho_{n\sigma}(\vec{r}-\vec{R}_v)$ by

$$\rho_{nm\sigma}(\vec{r}-\vec{R}_v)=|w_{nm\sigma}(\vec{r}-\vec{R}_v)|^2$$

(39)

and include the index m in the summation. Likewise the SIC potential for the WF, $V_{nm\sigma}^{SIC}(\vec{r}-\vec{R}_v)$, is given by Eq. (24) upon replacing $\rho_{n\sigma}$ by $\rho_{nm\sigma}$. The SIC-SCF equations for the Bloch states of a composite band are

$$[H_0+\Delta V_{ns\sigma\vec{k}}^{SIC}(\vec{r})]\psi_{ns\sigma\vec{k}}(\vec{r})=\sum_{n',s'}\epsilon_{n's'\vec{k},ns\vec{k}}\psi_{n's'\sigma\vec{k}}(\vec{r}),$$

(40)

where

$$\Delta V_{ns\sigma\vec{k}}^{SIC}(\vec{r})=\sum_{v,m}\Theta_{nsm\sigma\vec{k}}(\vec{r}-\vec{R}_v)V_{nm\sigma}^{SIC}(\vec{r}-\vec{R}_v),$$

(41)

$$\Theta_{nsm\sigma\vec{k}}(\vec{r}-\vec{R}_v)=N^{-1/2}e^{i\vec{k}\cdot\vec{R}_v}w_{nm\sigma}(\vec{r}-\vec{R}_v)$$

$$\times U_{s,m}^{\dagger}(\vec{k})/\psi_{ns\sigma\vec{k}}(\vec{r}).$$

(42)

The nondiagonal Lagrange multiplier $\epsilon_{n's'\vec{k},ns\vec{k}}$ vanishes if the ns and $n's'$ states are orthogonal by symmetry.

B. SIC for conduction bands

The theory developed in the preceding section applies to occupied bands of nonmetals. To address the question of SIC for conduction bands (CB), one must first specify the theoretical model used to describe the CB states. If the CB's are defined as the eigenstates of an extra electron added to the ground-state crystal of N electrons to form an $(N+1)$-electron system, as often done in the literature,[18] then there is no SIC for the CB since the extra electron sees all N electrons in the crystal. The bottom of the CB as defined by this $(N+1)$-electron model is identified with the electron affinity. However, in the context of op-

tical experiments, the CB are generally associated with excitation of an electron from the valence band (VB). This model differs from the earlier one as the excited electron now sees $N-1$ electrons. In the conventional energy-band theory the Coulomb potential for the *excited electron* is taken as that due to all N electrons of the unexcited crystal rather than the $N-1$ unexcited electrons of the excited crystal. The appropriate correction in this case is the Coulomb and exchange potential of the hole in the VB. Thus a knowledge of the hole density is needed to determine ΔV^{SIC} for the CB states. It is customary to regard the manifold of excited levels as a set of exciton-type discrete levels plus a continuum. If we accept the common assertion that a continuum excited state is one of complete delocalization which allocates $1/N$ of a hole to each atom,[19] then ΔV^{SIC} can be set to zero. This is analogous to the case of uncorrelated electron-hole behavior. However, the case of a partially localized hole (or electron)[20] must be considered in a more complete treatment. To make the appropriate correction for the case of partial localization, one would have to determine the density of the hole left behind by the excited electron. This entails a description beyond the one-electron band picture. The SIC for a partially localized CB might not be zero but should be much smaller than the SIC for the localized VB. Thus in this paper we adopt the approximation of complete delocalization and take ΔV^{SIC} as zero for CB. This approximation can be justified for large-gap ionic crystals because the VB states are so localized that the SIC for the energy-band gap is chiefly due to the SIC shift of the VB. For the case of semiconductors the validity of this approximation is not clear. Further studies of the SIC for CB states are in progress.

C. Unified Hamiltonian for all states

One complication introduced by the SIC is that the Hamiltonian is orbital dependent. For a given $\vec{k}$ different Hamiltonians must be solved for the core, VB, and CB states. Nevertheless, it is possible to obtain solutions for all states of a given $\vec{k}$ by diagonalizing a unified Hamiltonian with an operator technique similar to that employed in HF theory.[21] We define

$$P_i g \equiv \langle \psi_i | g \rangle \psi_i,$$

(43)

$$\hat{O}\equiv 1-\sum_i^{occ}P_i,$$

(44)

where the summation covers only the occupied orbitals of the ground state and the subscript i covers the $\vec{k}$, band, and spin indices. For the excited states ΔV^{SIC} is zero so that their Hamiltonian is no longer orbital dependent and is denoted by H_{exc} which is the same as the non-SIC LSD Hamiltonian. It has been shown[22] that the SIC-SCF equations given in Eqs. (30) and (40) for both the occupied and unoccupied states are identical to the eigenvalue equation

$$H_u\psi=E\psi$$

(45)

of the unified Hamiltonian,

$$H_u=\sum_i^{occ}(P_iH_iP_i+\hat{O}H_iP_i+P_iH_i\hat{O})+\hat{O}H_{exc}\hat{O},$$

(46)

with E corresponding to the diagonal Lagrange multipliers. This enables us to obtain the core, VB, and CB wave functions by diagonalizing the same Hamiltonian.

In the conventional LSD approximation the Koopmans theorem is not satisfied and the orbital energies no longer approximate the ionization energies well. However, it has been shown that the Koopmans theorem is approximately restored by the SIC, namely, the diagonal Lagrange multipliers ϵ_{ii} are much closer to the ionization energies than in the case of non-SIC LSD theory.[22] In this paper we adopt the diagonal Lagrange multipliers as the one-electron energies.

The nondiagonal multipliers can be determined from the appropriate wave functions as $\langle \psi_j | H_i | \psi_i \rangle$. When the "spherical approximation" of Sec. IV is used, nondiagonal multipliers arise only between levels from two bands that are separated by a forbidden gap, and are very small on account of the small overlap between the two wave functions involved. If the nondiagonal Lagrange multipliers are neglected, it can be shown that a simpler unified Hamiltonian

$$H_u = H_0 + \frac{1}{2} \sum_j (P_j \Delta V_j^{\text{SIC}} + \Delta V_j^{\text{SIC}} P_j) \qquad (47)$$

will suffice. Although our earlier work[14] was based on Eq. (47), in this paper we use the more exact form of Eq. (46). The VB energies of LiCl obtained by Eq. (46) and by Eq. (47) differ by typically 0.002 eV.

D. Matrix elements in LCAO representations

Although the unified Hamiltonian in Eq. (46) looks somewhat formidable, it turns out that with a linear combination of atomiclike orbitals (LCAO) basis set the ma-

trix elements associated with the SIC part of the Hamiltonian are no more difficult to evaluate than the non-SIC counterpart. Inclusions of SIC do not significantly increase the computational work. An outline of the methods for reducing the SIC matrix elements is described here.

If we take $H_{\text{exc}} = H_0$ as suggested in Sec. III B, Eq. (46) can be decomposed into

$$H_u = H_0 - \sum_{\substack{i,j \\ i \neq j}}^{\text{occ}} P_i H_0 P_j + \sum_i^{\text{occ}} (P_i \Delta V_i^{\text{SIC}} P_i + \hat{O} \Delta V_i^{\text{SIC}} P_i$$

$$+ P_i \Delta V_i^{\text{SIC}} \hat{O}) . \qquad (48)$$

Evaluation of LCAO matrix elements for H_0 has been discussed extensively in the literature and will not be detailed here.[12] The SIC potentials appear in the form of $\Delta V_i^{\text{SIC}} P_i$, $P_i \Delta V_i^{\text{SIC}}$, $P_j \Delta V_i^{\text{SIC}} P_i$, and $P_i \Delta V_i^{\text{SIC}} P_j$. To determine the SIC band structure by the LCAO method, we need matrix elements of the SIC terms between two Bloch-sum basis functions b_α which are linear combinations of atomiclike functions ϕ_α over all sites,

$$b_\alpha(\vec{k}, \vec{r}) = N^{-1/2} \sum_\nu e^{i\vec{k} \cdot \vec{R}_\nu} \phi_\alpha(\vec{r} - \vec{R}_\nu) . \qquad (49)$$

It is convenient to write P_i as $| \psi_i \rangle \langle \psi_i |$ so that

$$\langle b_\alpha | \Delta V_i^{\text{SIC}} P_i | b_\beta \rangle = \langle b_\alpha | \Delta V_i^{\text{SIC}} | \psi_i \rangle \langle \psi_i | b_\beta \rangle . \qquad (50)$$

As shown in Eqs. (41) and (42), ΔV_i^{SIC} contains ψ_i in the denominator. This just cancels the ψ_i in the right-hand index of $\langle b_\alpha | \Delta V_i^{\text{SIC}} | \psi_i \rangle$. Substitution of Eq. (49) leads to

$$\langle b_\alpha | \Delta V_i^{\text{SIC}} P_i | b_\beta \rangle = \sum_\nu e^{-i\vec{k} \cdot \vec{R}_\nu} \langle \phi_\alpha(\vec{r} - \vec{R}_\nu) | \sum_m V_{nm\sigma}^{\text{SIC}}(\vec{r}) U_{sm}^\dagger(\vec{k}) w_{nm\sigma}(\vec{r}) \rangle \langle \psi_i | b_\beta \rangle , \qquad (51)$$

where $n, s, \sigma, \vec{k}$ are four indices covered by the single index i. The right-hand side (rhs) contains no lattice sum over V^{SIC} as opposed to the matrix elements of H_0 which includes a lattice sum of localized potentials. A similar reduction applies to the matrix elements of $P_i \Delta V_i^{\text{SIC}}$ if we replace ΔV_i^{SIC} (a real potential) by its complex conjugate. Matrix elements for other terms in H_u can be written as simple linear combinations of these primary elements.

IV. APPROXIMATE WANNIER FUNCTIONS AND THE SPHERICAL APPROXIMATION

The present SIC-LSD theory is based on the use of the WF's as the localized orbitals. However, direct calculation of the WF's from the Bloch orbitals is difficult because of the slow convergence of the $\vec{k}$ summation over $N^{-1/2} \exp(-i\vec{k} \cdot \vec{R}_\nu) \psi_{n\sigma\vec{k}}$. In this section we describe approximate versions of the WF's which will be used later in this work.

For large-gap insulators the ground-state charge density is localized and the WF's are atomiclike aside from a

small residual amplitude at the neighboring atoms to maintain site orthogonality. The simplest approximation is to replace the WF's by the atomic orbitals. This approximation is undoubtedly very good for core states. As it turns out, it works satisfactorily even for the VB of LiCl (see Sec. VII).

A more refined approximation was used in Ref. 14. We expand ψ by Bloch-sum functions b_i [Eq. (49)] as

$$\psi_{n\sigma\vec{k}}(\vec{r}) = \sum_i C_{n\sigma}^i(\vec{k}) b_i(\vec{k}, \vec{r})$$

$$= N^{-1/2} \sum_\nu e^{i\vec{k} \cdot \vec{R}_\nu} \left[\sum_i C_{n\sigma}^i(\vec{k}) \phi_i(\vec{r} - \vec{R}_\nu) \right] . \qquad (52)$$

The last equation suggests a $\vec{k}$-dependent localized function,

$$u_{n\sigma\vec{k}}(\vec{r} - \vec{R}_\nu) = \sum_i C_{n\sigma}^i(\vec{k}) \phi_i(\vec{r} - \vec{R}_\nu) . \qquad (53)$$

The total density is the sum of all orbital densities in either the localized or delocalized representation, and thus,

for the case of a simple band,

$$\sum_v |w_{n\sigma}(\vec{r}-\vec{R}_v)|^2 = \sum_{\vec{k}} |\psi_{n\sigma\vec{k}}(\vec{r})|^2$$

$$= \sum_{\vec{k},v} N^{-1/2} e^{i\vec{k}\cdot\vec{R}_v} u_{n\sigma\vec{k}}(\vec{r}-\vec{R}_v)$$

$$\times \psi^*_{n\sigma\vec{k}}(\vec{r})$$

$$= \sum_v \eta_{n\sigma}(\vec{r}-\vec{R}_v) . \qquad (54)$$

We notice a certain similarity between the Wannier charge density and the "η local density" defined by

$$\eta_{n\sigma}(\vec{r}-\vec{R}_v)=N^{-1/2}\sum_{\vec{k}} e^{i\vec{k}\cdot\vec{R}_v} u_{n\sigma\vec{k}}(\vec{r}-\vec{R}_v)\psi^*_{n\sigma\vec{k}}(\vec{r}) .$$

$$(55)$$

In Appendix B we show that for a narrow band the Wannier charge density and the η local density are approximately equivalent and that each encloses one unit of charge. In calculating the WF's directly from $\exp(-i\vec{k}\cdot\vec{R}_v)\psi_{n\sigma\vec{k}}$, a very large number of $\vec{k}$ terms are needed in order to convert the delocalized $\psi_{n\sigma\vec{k}}$ functions into a localized one. On the other hand, each term on the rhs of Eq. (55) is localized because of the $u_{n\sigma\vec{k}}$ factor; thus the $\vec{k}$ summation converges rapidly, making $\eta_{n\sigma}$ much easier to calculate than the WF. Hence we approximate the Wannier charge density $\rho_{n\sigma}$ in Eq. (22) by $\eta_{n\sigma}$. As shown in Appendix C, minimization of the total-energy functional leads to

$$V_{n\sigma}^{SIC}(\vec{r}-\vec{R}_v)=-\int \eta_{n\sigma}(\vec{r}'-\vec{R}_v)|\vec{r}-\vec{r}'|^{-1}d\vec{r}'$$

$$+V_{xc,\sigma}[\eta_{n\sigma}(\vec{r}-\vec{R}_v),0] , \qquad (56)$$

$$\Delta V_{n\sigma\vec{k}}^{SIC}=N^{-1/2}\sum_v e^{i\vec{k}\cdot\vec{R}_v} u_{n\sigma\vec{k}}(\vec{r}-\vec{R}_v)$$

$$\times V_{n\sigma}^{SIC}(\vec{r}-\vec{R}_v)/\psi_{n\sigma\vec{k}}(\vec{r}) . \qquad (57)$$

This is equivalent to replacing $\rho_{n\sigma}$ by $\eta_{n\sigma}$ in Eq. (24) and replacing $w_{n\sigma}$ by $u_{n\sigma\vec{k}}$ in Eq. (29).

For a composite band with a subband Bloch wave $\psi_{ns\sigma\vec{k}}$, we form $u_{ns\sigma\vec{k}}$ and $\eta_{ns\sigma}$ following the steps of Eqs. (53) and (55). Through the matrix $U(\vec{k})$ defined in Eq. (38), we transform $\psi_{nm\sigma\vec{k}}$ into symmetry-adapted Bloch waves $\psi_{nm\sigma\vec{k}}$ and then determine $u_{nm\sigma\vec{k}}$ and $\eta_{nm\sigma}$ which are to approximate the corresponding WF and Wannier charge density. One problem is that for an arbitrary $\vec{k}$ point the $U(\vec{k})$ matrix is rather difficult to compute. By adopting an averaging procedure similar to that used in atomic structure theory, we are able to bypass the calculation of the $U(\vec{k})$ matrix in the following way. For an atom with an open shell of $l\neq0$, the Coulomb potential, in general, is not spherically symmetrical and may depend on the magnetic quantum numbers of the orbital. It is customary to average the potential over the magnetic quantum number. This results in a common spherically symmetric potential for all magnetic sublevels and is usually referred to as the spherical approximation. In our present problem this spherical approximation consists in summing $\eta_{nm\sigma}$ over all m and dividing by the number of subbands n_s,

$$\bar{\eta}_{n\sigma}(\vec{r}-\vec{R}_v)\equiv n_s^{-1}N^{-1/2}$$

$$\times \sum_{\vec{k},m} e^{i\vec{k}\cdot\vec{R}_v} u_{nm\sigma\vec{k}}(\vec{r}-\vec{R}_v)\psi^*_{nm\sigma\vec{k}}(\vec{r})$$

$$=n_s^{-1}N^{-1/2}\sum_{\vec{k},s} e^{i\vec{k}\cdot\vec{R}_v} u_{ns\sigma\vec{k}}(\vec{r}-\vec{R}_v)\psi^*_{ns\sigma\vec{k}}(\vec{r}) .$$

$$(58)$$

The last step follows from the fact that $u_{nm\sigma\vec{k}}$ and $\psi_{nm\sigma\vec{k}}$ are related, respectively, to $u_{ns\sigma\vec{k}}$ and $\psi_{ns\sigma\vec{k}}$ through the same unitary transformation $U(\vec{k})$. The spherical approximation enables us to use, for all subbands of a given composite band, a common $\bar{\eta}_{n\sigma}$ which is determined directly from $\psi_{ns\sigma\vec{k}}$ without transforming to $\psi_{nm\sigma\vec{k}}$. Under the spherical approximation the local SIC potential for a composite band is an m-independent average one, $\bar{V}_{n\sigma}^{SIC}(\vec{r}-\vec{R}_v)$, obtained by inserting $\bar{\eta}_{n\sigma}$ in Eq. (56), and the periodic ΔV^{SIC} for the composite band is

$$\Delta V_{ns\sigma\vec{k}}^{SIC}(\vec{r})=N^{-1/2}\sum_v e^{i\vec{k}\cdot\vec{R}_v} u_{ns\sigma\vec{k}}(\vec{r}-\vec{R}_v)\bar{V}_{n\sigma}^{SIC}(\vec{r}-\vec{R}_v)/\psi_{ns\sigma\vec{k}}(\vec{r}) . \qquad (59)$$

This leads to the simplification

$$\langle b_\alpha | \Delta V_i^{SIC}P_i | b_\beta \rangle = \sum_v e^{-i\vec{k}\cdot\vec{R}_v}\langle \phi_\alpha(\vec{r}-\vec{R}_v) | \bar{V}_{n\sigma}^{SIC}(\vec{r})u_{ns\sigma\vec{k}}(\vec{r})\rangle\langle \psi_{ns\sigma\vec{k}} | b_\beta \rangle . \qquad (60)$$

For the Ar and LiCl crystals a measure of the error of the spherical approximation may be taken as the difference between the matrix elements $\langle \phi_{3px}(\vec{r}) | V_{3px}^{SIC}(\vec{r}) | \phi_{3px}(\vec{r})\rangle$ and $\langle \phi_{3px}(\vec{r}) | \bar{V}_{3p}^{SIC}(\vec{r}) | \phi_{3px}(\vec{r})\rangle$. Our calculation shows a 1.5% difference for Ar and 5% for LiCl.

V. APPLICATION TO ARGON

A. Non-SIC energy-band calculation

The Ar crystal is a face-centered-cubic (fcc) structure with a lattice constant $a=10.05$ a.u. and has inversion symmetry about an Ar site. Placing the origin on an Ar site, we write a Bloch-sum basis function as

$$b_j(\vec{k},\vec{r})=N^{-1/2}\Delta_j\sum_v e^{i\vec{k}\cdot\vec{R}_v}\phi_j(\vec{r}-\vec{R}_v) , \qquad (61)$$

where

$$\Delta_j = \exp(\tfrac{1}{2} i n_j \pi) , \tag{62}$$

with n_j being 0, 1, and 2 for the s-, p-, and d-type orbitals, respectively. The choice of the phase factor Δ_j ensures that the matrix elements are real. The atomiclike functions ϕ_j are atomic orbitals expanded in Gaussian-type orbitals (GTO's), e.g.,

$$\phi = \sum_i a_i e^{-\beta_i r^2} , \quad \sum_i a_i x e^{-\beta_i r^2} , \tag{63}$$

etc., or single Gaussians. We include in the basis set ϕ the wave functions for all occupied orbitals of the free Ar atom calculated using a SCF atomic program modified to include SIC and expanded in the Gaussian form with $\beta_i = 4027.3$, 1144.96, 376.954, 138.07, 54.954, 18.6119, 7.436 92, 3.088 57, 1.102 67, 0.650 663, 0.414 763, 0.145 449, and 0.053. These exponents were selected mostly from those of Veillard[23] to accurately reproduce the free-atom wave functions. For the remainder of the basis set a sufficient number of single-Gaussian Bloch sums are utilized to maintain a high degree of variational freedom. The use of three additional s-type GTO's (3.088 57, 0.650 663, and 0.053) and p-type GTO's (1.102 67, 0.414 763, and 0.053) lead to good convergence of all the occupied bands. For the CB an extended basis set is required; in addition to the basis functions cited earlier two more s-type GTO's (0.414 763 and 0.145 449), two p-type GTO's (0.650 663 and 0.145 449), an atomic $3d$ wave function, and two d-type GTO's (0.650 663 and 0.145 449) are employed.

To begin the SCF energy-band calculation, the zeroth-order approximation to the crystal charge density is made from the overlapping atomic charge (OAC)

$$\rho_{\text{crystal}}^{(0)}(\vec{r}) = \sum_\nu \rho_a(\vec{r} - \vec{R}_\nu) , \tag{64}$$

where ρ_a is the atomic charge density. For the non-SIC problem we drop the spin index σ since there is no spin polarization. The zeroth-order Coulomb potential $V_C^{(0)}$ is generated by directly integrating the rhs of Eq. (64). The LDF exchange potential (spin-unpolarized) is

$$V_X = [(6/\pi)\rho_\sigma(\vec{r})]^{1/3} = [(3/\pi)\rho_{\text{crystal}}(\vec{r})]^{1/3} . \tag{65}$$

In order to cast the crystal potential V_{crystal} (which is $V_C + V_X$) in a form suitable for energy calculation, we compute $V_{\text{crystal}}^{(0)}$ at 212 nonequivalent points in a unit cell and then least-squares-fit the result to a lattice superposition of localized functions, e.g.,

$$V_{\text{crystal}}^{(0)}(\vec{r}) = \sum_\nu f(\vec{r} - \vec{R}_\nu) . \tag{66}$$

As a functional form of f, we choose a multipole expansion in terms of spherical harmonics Y_{lm} and retain all terms up to $l = 4$. For local cubic symmetry the terms with $l = 1-3$ are excluded and f has the form

$$f(\vec{r}) = w(r) + (x^4 + y^4 + z^4 - 3r^4/5)w'(r) , \tag{67}$$

where $w(r)$ and $w'(r)$ are expressed as series of $\exp(-\omega_i r^2)$ and $r^2 \exp(-\omega_j' r^2)$ through curve fitting.

Since Ar is a crystal of weakly bound atoms, throughout the SCF procedure the $l = 4$ component makes a minimal contribution, but is retained to ensure convergence of the multipole expansion and to guard against any unexpectedly large charge distortion due to inclusion of SIC. With the use of this Gaussian representation of $V_{\text{crystal}}^{(0)}$, we compute all the overlap and non-SIC Hamiltonian matrix elements with the Bloch-sum basis functions using analytic Gaussian techniques described in the literature.[12,24] The secular equations are solved at four high-symmetry $\vec{k}$ points (Γ, X, L, W).

In Eq. (64) the local decomposition for the zeroth-iteration crystal charge density was established by the atomic charge distribution. For the first iteration the local decomposition may be established by the Wannier charge densities, i.e.,

$$\rho_{\text{crystal}}^{(1)}(\vec{r}) = 2 \sum_{n,m,\nu} |w_{nm}(\vec{r} - \vec{R}_\nu)|^2 . \tag{68}$$

Alternatively, the eigenfunctions resulting from the solution of the secular equations at four $\vec{k}$ points are used to generate the crystal charge density at 212 nonequivalent points and least-squares fit into a lattice superposition of localized functions

$$\rho_{\text{crystal}}^{(1)}(\vec{r}) = \sum_\nu g(\vec{r} - \vec{R}_\nu) , \tag{69}$$

$$g(\vec{r}) = h(r) + (x^4 + y^4 + z^4 - 3r^4/5)h'(r) , \tag{70}$$

where $h(r)$ and $h'(r)$ are expressed as mixtures of exponential functions $\exp(-\mu_i r)$ and $r^2 \exp(-\mu_j' r)$. In fitting Eq. (69) we have found it advantageous to place the following constraint. If we Fourier-analyze the crystal potential

$$V_{\text{crystal}}(\vec{r}) = \sum_\mu V(\vec{K}_\mu) \cos(\vec{K}_\mu \cdot \vec{r}) , \tag{71}$$

where $\vec{K}_\mu$ are the reciprocal-lattice vectors, the Fourier component for $\vec{K}_\mu = 0$ is related to the WF as

$$V(\vec{K}_\mu = 0) = -\frac{4\pi}{3\Omega} \sum_{n,m} \int |w_{nm}(\vec{r})|^2 r^2 d\vec{r} , \tag{72}$$

where Ω is the volume of a Wigner-Seitz (WS) cell. In our case the integral is evaluated directly from the η localized densities (determined from ψ),

$$V(\vec{K}_\mu = 0) = -\frac{4\pi}{3\Omega} \sum_n n_s \int \bar{\eta}_n(\vec{r}) r^2 d\vec{r} . \tag{73}$$

We require that this value be reproduced in fitting the charge density, i.e.,

$$V(\vec{K}_\mu = 0) = -\frac{2\pi}{3\Omega} \int g(\vec{r}) r^2 d\vec{r} . \tag{74}$$

Here the multiplicative factor is reduced to $2\pi/3\Omega$ because of the factor of 2 which appears in Eq. (68) but not in Eq. (69). With $\rho_{\text{crystal}}^{(1)}$ in the form of either Eq. (68) or (69), we are able to repeat the iteration cycle and reach self-consistency. A partial listing of the non-SIC band structures is given in Table I, and curves for the VB and CB are shown in Fig. 1.

TABLE I. Band gap, VB width, and core levels of solid argon calculated by LSD and by SIC-LSD. Core-level energies are referenced to the centroid of the VB. Experimental values (see second paragraph, Sec. V C) are included for comparison. All energies are in units of eV.

	LSD[a]	SIC-LSD[a]	Expt.[b]	SIC-LSD[c]
Band gap	7.89	13.9	14.2	13.5
VB width	1.36	1.23	1.3—1.7	1.21
$E(1s)$	−3080	−3200		−3201
$E(2s)$	−282	−300		−300
$E(2p)$	−218	−241	−234	−241
$E(3s)^d$	−13.4	−14.2	~ −13	−14.2

[a]Using the $\rho^{1/3}$ exchange.

[b]See the second paragraph in Sec. V C.

[c]Using the $\rho^{1/3}$ exchange and the correlation potential of Ref. 38.

[d]Energy refers to the centroid of the 3s core band.

B. SIC calculation

For a given $\vec{k}$ point one must determine the SIC potential for each occupied band in order to construct the unified Hamiltonian. Our procedure is to use the SCF non-SIC crystal wave functions from the preceding subsection as the starting point for calculating the approximate Wannier charge densities $\eta_{n\sigma}(\vec{r}-\vec{R}_\nu)$ from which we determine $V^{SIC}_{n\sigma}(\vec{r}-\vec{R}_\nu)$ and then the matrix elements of H_u as explained in Sec. III D. The solutions of H_u are then iterated to self-consistency. Typically this requires only two or three cycles.

Applying the spherical approximation to the p bands, we determine η_{1s}, η_{2s}, $\bar{\eta}_{2p}$, η_{3s}, and $\bar{\eta}_{3p}$ as described in Eqs. (55) and (58). Here the spin index is deleted since the same function applies to both spins. We find η_{1s}, η_{2s}, and $\bar{\eta}_{2p}$ to be virtually identical to the respective atomic charge densities as may be expected of deep core-state bands. The numerical values of the η_n functions are computed at 100 points for the deep core states and 600 points for the remainder of bands so as to fit these functions to a sum of exponential terms $\exp(-\alpha r)$ and $r^2\exp(-\alpha r)$. Be-

sides demanding each fit to enclose one unit of charge, an additional constraint is imposed on each fit to preserve the value of $\langle r^2 \rangle$ which is calculated analytically from Eqs. (55) and (58). The $\bar{V}^{SIC}_n(\vec{r}-\vec{R}_\nu)$ for each band is tabulated at the same points as before and refitted to the following Gaussian form:

$$\bar{V}^{SIC}_n(\vec{r})=r^{-1}(e^{-\alpha r^2}-1)+\sum_i A_i e^{-\alpha_i r^2}+\sum_j A'_j r^2 e^{-\alpha_j r^2}.$$

(75)

The first term reproduces the correct r^{-1} dependence at large distances. A good fit is obtained using only single-center functions. The matrix elements of the SIC part of the unified Hamiltonian of Eq. (48) are exemplified by Eq. (60). Since $u_{n\sigma\vec{k}}(\vec{r})$ are simply related through Eq. (53) to the atomiclike orbitals ϕ_i which are in Gaussian form, the use of Eq. (75) allows us to decompose

$$\langle \phi_\alpha(\vec{r}-\vec{R}_\nu) \mid \bar{V}^{SIC}_n(r)u_{n\sigma\vec{k}}(\vec{r}) \rangle$$

into a series of two-center Gaussian integrals which can be computed easily. Diagonalization of H_u yields a new set of ψ's with which we recompute the SIC matrix elements to complete the iteration cycle and reach self-consistency. The SIC band structure is shown in Fig. 2.

C. Results

In the first two columns of Table I we list the energy-band gap, VB width, and the core levels (relative to the centroid of the VB) of the argon crystal obtained by the SIC-LSD and LSD (no SIC) calculations. For comparison the experimental values are also included.[25−29] The improvement in band gap by the SIC is evident; it increases the uncorrected LSD value of 7.9 to 13.9 eV in good agreement with the experimental value of 14.2 eV. The effect of SIC on the VB width, however, is much smaller. Comparison of Fig. 1 with Fig. 2 also indicates that the VB structure is not greatly altered by the SIC. The calculated density of states (DOS) of the VB for the LSD-SIC results is shown in Fig. 3 and is in good agreement with experimental data.[26] The centroid of the VB is 0.57 eV
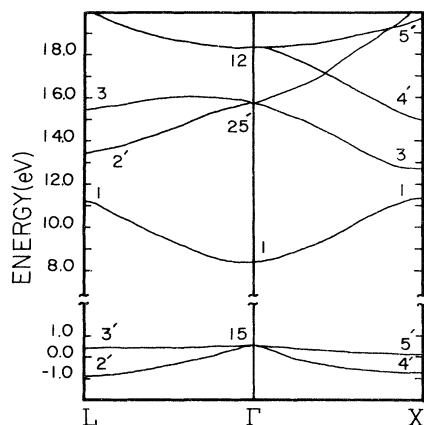
FIG. 1. VB's and CB's of the Ar crystal calculated by LSD (without SIC). Centroid of the VB is set to zero energy.
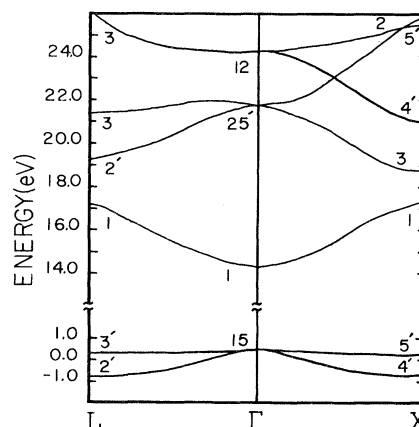
FIG. 2. VB's and CB's of the Ar crystal calculated by SIC-LSD. Centroid of the VB is set to zero energy.
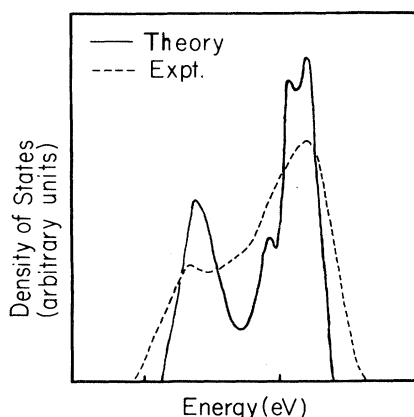
FIG. 3. DOS for the VB of the Ar crystal (solid curve) and experimental photoelectron spectrum (dashed curve) of Ref. 26. Zero of the energy scale is arbitrary.

below the upper edge.

The core levels are also lowered by the SIC. The calculated core energies in Table I are referenced to the VB centroid, thus the change in core levels from LSD to SIC-LSD reflects the difference in SIC shifts between the cores and the VB. The experimental core levels for argon in Table I were taken from the results of soft-x-ray analysis of the core region.[25,27−29] The interband edge was placed 3.0 eV from the $L_{\mathrm{II,III}}$ soft-x-ray threshold based on a recent detailed calculation[30] of the localized excitonic structure. Therefore the experimental energy of the $2p$ core level can be accurately placed 234 eV below the VB centroid. This compares to a somewhat deeper SIC-LSD value of -241 eV. For the free Ar atom the absolute value of the SIC-LSD $2p$ orbital energy is 5.5 eV larger than the measured ionization energy. When this is taken into account, the agreement is excellent. The interband edge for the $3s$ core transitions is placed at the soft-x-ray threshold since a theoretical analysis of the excitonic character is unavailable. For the $3s$ level which is a shallow core state, the maximum excitonic binding energy associated with a localized transition to the CB is likely smaller than the value associated with the deeper core states. Therefore the experimental uncertainty is estimated as about .2 eV (the maximum excitonic binding energy associated with the VB photoabsorption). The SIC-LSD orbital $3s$ energy lies at -14.2 eV and is within experimental uncertainty of the experimental value of -13.2 eV.

Several band-structure calculations for solid argon employing the HF approximation have been reported in the literature. Lipari and Fowler[31] (LF) determined the band structure using the orthogonalized-plane-wave (OPW) method. They presented the HF results and an important analysis of how correlation applies to HF crystal calculations. Lipari[32] (L) later repeated the HF calculation using a mixed basis set. Dagens and Perrot[33] (DP) presented the findings of an application of the augmented-plane-wave (APW) method in which they made effective use of a muffin-tin approximation. Another treatment based on a tight-binding formalism was offered by Kunz and Mick-

ish (KM).[34] More recently Baroni, Grosso, and Pastori Parravicini[35] (BGPP) used the OPW method with a limited Gaussian basis set in a calculation where all the matrix elements were calculated in an analytic form. Briefly the results compare as follows: LF, L, DP, KM, and BGPP reported 17.0, 16.4, 18.5, 18.5, and 17.9 eV, respectively, for a HF band gap and 2.3, 2.6, 1.2, 1.3, and 1.9 eV, respectively, for a HF VB width. Furthermore, correlation has been included in the works of LF and KM in a semiempirical manner. LF reported a lowering of the band gap to 13.7 eV and KM found a similar shift in the bandgap to 15.2 eV and a slight narrowing of the VB width to 1.2 eV. These results compare to our predicted band gap of 13.9 eV and VB width of 1.23 eV. It is interesting to note that our results compare best with the correlated HF results. In addition to the CB edge and VB structure, considerable interest exists as to the position of the d-state continuum in the CB. The Γ'_{25c}-Γ_{1c} and Γ_{12c}-Γ_{1c} spacings (the subscript c for CB) reported by LF, L, and KM are 10.4 and 12.9 eV, 9.85 and 12.7 eV, and 10.1 and 12.9 eV, respectively. Somewhat smaller separations are given in Refs. 33 and 35; i.e., 8.3 and 11.3 eV by DP and 8.6 and 12.1 eV by BGPP. Our calculated Γ'_{25c}-Γ_{1c} and Γ_{12c}-Γ_{1c} separations of 7.44 and 9.90 eV are in better agreement with the latter group which included the more recent HF calculation of BGPP. The smaller Γ'_{25c}-Γ_{1c} and Γ_{12c}-Γ_{1c} spacings from our calculation as compared to BGPP are consistent with a general trend across the CB structure in which our results are slightly compressed relative to the HF calculation.

The question of self-interaction has been addressed by Kunz et al. in Ref. 11. They give the self-interaction through the WF as

$$\int w_i^2(\vec{r}-\vec{R}_N)w_i^2(\vec{r}'-\vec{R}_N)\,|\,\vec{r}-\vec{r}'\,|^{\,-1}d\vec{r}\,d\vec{r}' \qquad (76)$$

and add, to the *Hartree* potential of an n-electron system, the following term

$$-\sum_{i=1}^{n}|\,\phi_i\,\rangle\left[\int\frac{w_i^2(\vec{r}-\vec{R}_N)w_i^2(\vec{r}'-\vec{R}_N)}{|\,\vec{r}-\vec{r}'\,|}d\vec{r}\,d\vec{r}'\right]\langle\,\phi_i\,|\ ,$$

$$(77)$$

where ϕ_i is a one-electron orbital. Consequently, the energies of the orbitals associated with the Wannier function w_i are shifted downward by the amount given in (76). The local exchange potential of Kohn and Sham and the screening potential of Robinson et al.[36] were initially adopted. (See Ref. 11 for more details of the treatment.) If we read the graph labeled as "Hartree and exchange correlation" in Fig. 2 of Ref. 11 to get the band gap,[37] we find a value of 15.2 eV which is slightly higher than our SIC-LSD value of 13.9 eV.

In our LSD-SIC work reported above, the Kohn-Sham "exchange-only" form was used as the exchange-correlation potential. The SIC formulation presented in this paper is not restricted to the $\rho^{1/3}$ exchange and other versions of the exchange-correlation density functional may be used. As an illustration we add to the $\rho^{1/3}$ exchange the correlation potential of von Barth and Hedin[38] and the resulting band structure of Ar is shown in the last

column of Table I. The band gap decreases by 0.4 eV as compared to the exchange-only calculation. Other forms of exchange-correlation potential have been used in the literature.[39] A comprehensive study of the effects of the various correlation functionals on the energy-band structure is deferred to a later paper.

VI. APPLICATION TO LITHIUM CHLORIDE

A. Non-SIC energy-band calculation

The crystal structure of LiCl consists of two interpenetrating fcc lattices with lattice constant $a = 9.7132$ a.u. separated by a nonprimitive translation $\vec{t} = \frac{1}{2}a(100)$. Placing the origin on an anion site, we write the Bloch-sum basis functions associated with the Cl and Li sites as

$$b_j^{\mathrm{Cl}}(\vec{k},\vec{r}) = N^{-1/2}\Delta_j \sum_\nu e^{i\vec{k}\cdot\vec{R}_\nu}\phi_j^{\mathrm{Cl}}(\vec{r}-\vec{R}_\nu) , \qquad (78)$$

$$b_j^{\mathrm{Li}}(\vec{k},\vec{r}) = N^{-1/2}\Delta_j \sum_\nu e^{i\vec{k}\cdot(\vec{R}_\nu+\vec{t})}\phi_j^{\mathrm{Li}}(\vec{r}-\vec{R}_\nu-\vec{t}) , \qquad (79)$$

where Δ_j is given in Eq. (62). The local basis set of ϕ^{Cl} and ϕ^{Li} contains atomic wave functions of all the occupied states of the free ions as well as single Gaussians. The atomic wave functions are expanded in Gaussian form with exponents $\beta_i = 1010.62$, 453.179, 150.796, 64.6268, 22.1381, 9.34746, 2.60863, 0.997212, 0.444620, 0.140120, and 0.050791 for Li, and $\beta_i = 105747$, 15855.3, 3615.32, 1030.03, 504.978, 132.121, 47.1522, 18.7012, 6.53287, 2.61988, 0.950083, 0.448205, 0.159272, and 0.075000 for Cl, taken from those of Harrison and Lin[40] to accurately reproduce the atomic wave functions obtained by a SCF-SIC-LSD calculation. We use four s-type (2.60863, 0.997212, 0.44462, and 0.14012) and four p-type (9.34746, 0.997212, 0.44462, and 0.14012) single Gaussians for Li along with three s-type and three p-type (0.448205, 0.159272, and 0.075) single Gaussians for Cl in order to ensure convergence of the occupied bands. To obtain an accurate solution for the lower part of the CB we introduce three extra d-type (0.997212, 0.44462, and 0.14012) single Gaussians for Li and an atomic $3d$ orbital plus two d-type single Gaussians (0.448205 and 0.159272) for Cl. As an initial approximation the crystal electron density is taken as the OAC form

$$\rho_{\mathrm{crystal}}^{(0)} = \sum_\nu [\rho(\mathrm{Cl}^- \mid \vec{r}-\vec{R}_\nu)+\rho(\mathrm{Li}^+ \mid \vec{r}-\vec{R}_\nu-\vec{t})] , \qquad (80)$$

where the two ρ's are the free-ion electron densities. The zeroth-order Coulomb potential energy is

$$V_C^{(0)}(\vec{r}) = V_{\mathrm{nuc}}(\vec{r})+V_{ee}^{(0)}(\vec{r}) , \qquad (81)$$

where $V_{\mathrm{nuc}}(\vec{r})$ is due to the fixed nuclei and V_{ee} is due to electron-electron Coulomb potential of ρ_{crystal}. Because of the ionic nature of the crystal, each site has a net charge of ± 1. Thus V_C contains a superposition of long-range r^{-1} tails from all sites, making the SCF calculation very tedious. To circumvent this problem we define V_{ion} as the Coulomb potential energy due to a positive charge at each

Li site and a negative charge at each Cl site,

$$V_{\mathrm{ion}}(\vec{r}) \equiv \sum_\nu (\mid \vec{r}-\vec{R}_\nu \mid^{-1} - \mid \vec{r}-\vec{R}_\nu-\vec{t} \mid^{-1}) , \qquad (82)$$

and rewrite Eq. (81) as

$$V_C(\vec{r}) = V_C'(\vec{r})+V_{\mathrm{ion}}(\vec{r}) , \qquad (83)$$

$$V_C'(\vec{r}) = V_{\mathrm{nuc}}(\vec{r})+V_{ee}(\vec{r})-V_{\mathrm{ion}}(\vec{r}) . \qquad (84)$$

V_C' is now devoid of the troublesome r^{-1} tails and is reconstructed each iteration from the new crystal charge density. The V_{ion} term does not involve the electron density, thus its matrix elements are computed one time using an Ewald-type procedure[41] and added to the matrix elements of V_C each iteration.

The LDF exchange potential is computed at 243 nonequivalent points in the unit cell and added to the Coulomb potential. The total potential is then curve-fitted to a lattice superposition

$$V_{\mathrm{crystal}}^{(0)} = \sum_\nu [f(\mathrm{Cl} \mid \vec{r}-\vec{R}_\nu)+f(\mathrm{Li} \mid \vec{r}-\vec{R}_\nu-\vec{t})] . \qquad (85)$$

The local site symmetry for both Cl and Li is cubic and $f(\vec{r})$ is chosen to have the same functional form given in Eq. (67). The $l=4$ component is found to make a minimal contribution. Throughout the SCF procedure the local aspherical character is small. The secular equations are solved at four high-symmetry $\vec{k}$ points (Γ,X,L,W) to generate a new charge density. The SCF iteration procedure is similar to that described in Sec. V A.

B. SIC calculation

The SIC formulation presented in Sec. III is for monatomic crystals. A slight modification must be made to extend it to diatomic crystals. Since the crystal wave function is expanded by Bloch sums of Li-centered orbitals and of Cl-centered orbitals [Eqs. (78) and (79)], each subband wave function can be cast in the form

$$\psi_{ns\vec{k}}(\vec{r}) = N^{-1/2}$$

$$\times \sum_\nu e^{i\vec{k}\cdot\vec{R}_\nu}[v_{ns\vec{k}}(\mathrm{Cl} \mid \vec{r}-\vec{R}_\nu)$$

$$+ e^{i\vec{k}\cdot\vec{t}}v_{ns\vec{k}}(\mathrm{Li} \mid \vec{r}-\vec{R}_\nu-\vec{t})] , \qquad (86)$$

where the v's are localized functions centered at the appropriate site and can be determined directly from the LCAO solution of $\psi_{ns\vec{k}}$. For SIC work we seek to express $\psi_{ns\vec{k}}$ as

$$\psi_{ns\vec{k}}(\vec{r}) = N^{-1/2}\sum_\nu e^{i\vec{k}\cdot\vec{R}_\nu}u_{ns\vec{k}}(\vec{r}-\vec{R}_\nu) . \qquad (87)$$

Letting $\vec{t}_1$, $\vec{t}_2,\ldots,\vec{t}_6$ be $\frac{1}{2}a(\pm 100)$, $\frac{1}{2}a(0\pm 10)$, $\frac{1}{2}a(00\pm 1)$, we see that it is possible to bring Eq. (86) to the form of Eq. (87) by setting

$$u_{ns\vec{k}}(\vec{r})=v_{ns\vec{k}}(\text{Cl}\,|\,\vec{r})+\tfrac{1}{6}\sum_{i'=1}^{6}e^{i\vec{k}\cdot\vec{t}_{i'}}v_{ns\vec{k}}(\text{Li}\,|\,\vec{r}-\vec{t}_{i'})$$

(88)

for Cl bands, and

$$u_{ns\vec{k}}(\vec{r})=v_{ns\vec{k}}(\text{Li}\,|\,\vec{r})+\tfrac{1}{6}\sum_{i'=1}^{6}e^{i\vec{k}\cdot\vec{t}_{i'}}v_{ns\vec{k}}(\text{Cl}\,|\,\vec{r}-\vec{t}_{i'})$$

(89)

for Li bands. This form of $u_{ns\vec{k}}$ ensures the correct local symmetry for the η local densities determined from Eqs. (88) and (89). For the deep core states the η's are found to be virtually identical to their atomic counterparts. The numerical values of the η's are fitted with a sum of exponential functions like $\exp(-\alpha r)$ and $r^2\exp(-\alpha r)$ at typically 100 points for the deep core states and 600 points for the remaining bands. For the VB and the Cl $3s$ band, the contributions from the $v_{ns\vec{k}}(\text{Li}\,|\,\vec{r}-\vec{t}_i)$ terms in Eq. (88) to the η local densities are so small that a good fit for the latter is achieved using only single-center terms. Dual constraints are imposed on the fit by demanding the fit to enclose one unit of charge and to preserve the value of $\langle r^2\rangle$ calculated directly using Eqs. (55) and (58). The V^{SIC} for each band is tabulated at the same points used previously and refitted to the Gaussian form of Eq. (75). The required matrix elements are computed and H_u is constructed. This procedure is repeated and the SIC potential and the non-SIC crystal potential matrix elements are computed each iteration until self-consistency is reached.

C. Results

The band gap, VB width, and core levels calculated with and without SIC are presented in the first two columns of Table II along with the experimental values.[42-51] The last column gives the values calculated with the $\rho^{1/3}$ exchange and the correlation potential of von Barth and Hedin.[38] Again the SIC improves the band gap remarkably but has much smaller effects on the VB

width. With the $\rho^{1/3}$ exchange the calculated band gap is about 1 eV above the experimental value, but inclusion of correlation brings the calculated band gap to within a few tenths of an eV of the experimental value. Figures 4 and 5 show, respectively, the LSD and SIC-LSD energy-band diagrams. The VB structure is not significantly altered by the SIC. The VB DOS of the SIC-LSD band structure is shown in Fig. 6 and agrees with the photoelectron spectra.[45] The centroid of the VB is 1.4 eV below the upper edge.

The core-level energies are significantly improved by the SIC as is evident in Table II. The experimental position of the Cl $3s$ level has been measured by x-ray photoelectron spectroscopy (XPS).[47] This places the $3s$ level 12.0 eV below the VB centroid in very good agreement with our SIC-LSD result of 12.3 eV. Another XPS experiment places the $3s$ level at -10.5 eV, but the authors regard their LiCl data as unreliable because of surface contamination by water.[50] For the Cl $2p$ level we take the Cl^- $L_{\text{II,III}}$ soft-x-ray threshold and estimate the interband edge to be 3 eV above it based on the results of an excitonic calculation[30] of the Ar $L_{\text{II,III}}$ referred to in Sec. V C. This analysis places the Cl $2p$ core level 194 eV below the VB centroid with an uncertainty of ± 1 eV. The SIC-LSD prediction is -201 eV. The discrepancy of 7 eV is consistent with the 6-eV difference between the SIC free-atom $2p$ level and experiment. As to the Li $1s$ band our SIC-LSD calculation gives -54.6 eV (relative to the VB centroid) as compared to -51.7 eV from experiment.[51] The discrepancy of 3 eV cannot be explained in a simple free-atom argument, as the SIC-LSD atomic orbital energy differs by only 0.3 eV from the observed ionization energy. One possible explanation might be an unusually large orbital relaxation occurring around the hole left in the Li $1s$ band due to the poor screening of the hole by the Li^{2+} ion.

Only a limited number of calculations employing the HF method have been published for the LiCl crystal. Kunz has reported HF results and also HF calculations with correlation.[52-54] In Ref. 54 a HF band gap of 16.8 eV is given, but correlation reduces the band gap to 9.7 eV. The VB width (with correlation) is 3.6 eV. Perrot[55]

TABLE II. Band gap, VB width, and core levels of the LiCl crystal calculated by LSD and by SIC-LSD. Core-level energies are referenced to the centroid of the VB. Experimental values (see second paragraph, Sec. VI C) are included for comparison. All energies are in units of eV.

	LSD[a]	SIC-LSD[b]	Expt.[b]	SIC-LSD[c]
Band gap	5.81	10.9	9.4–9.9	10.1
VB width	3.07	2.93	~3.6	2.87
E(Li $1s$)	−40.7	−54.6	−51.7	−54.7
E(Cl $1s$)	−2714	−2829		−2829
E(Cl $2s$)	−239	−256		−256
E(Cl $2p$)	−181	−201	−194	−202
E(Cl $3s$)[d]	−11.1	−12.3	−12.0	−12.3

[a]Using the $\rho^{1/3}$ exchange.
[b]See the second paragraph in Sec. VI C.
[c]Using the $\rho^{1/3}$ exchange and the correlation potential of Ref. 38.
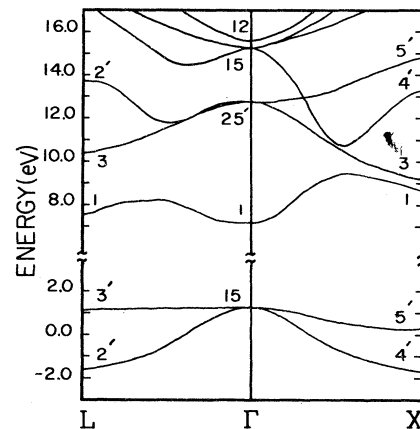[d]Energy refers to the centroid of the $3s$ core band.

FIG. 4. VB's and CB's of the LiCl crystal calculated by LSD (without SIC). Centroid of the VB is set to zero energy.
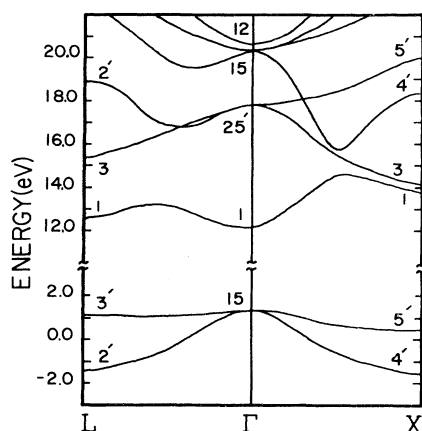
FIG. 5. VB's and CB's of the LiCl crystal calculated by LSD. Centroid of the VB is set to zero.

also studied LiCl using the APW method with a muffin-tin approximation and found the HF band gap to lie at 15.5 eV with a VB width of 2.64 eV. He also included correlation effects which lowered the band gap to 8.5 eV. These results may be compared to our predicted band gap of 10.1 and 10.9 eV (with and without correlation) and a VB width of 2.87 and 2.93 eV. For the CB, Kunz's work shows 8.3 eV for the Γ'_{25}-Γ_{1c} spacing[54] and 10.6 eV for[52] Γ_{12c}-Γ_{1c}, whereas smaller values (5.2 and 8.2 eV) are found by Perrot[55] in his correlated HF calculation. This compares to our value of 5.6 eV for Γ'_{25c}-Γ_{1c} and 8.3 eV for Γ_{12c}-Γ_{1c}. The larger values reported by Kunz are consistent with the larger spacings he found for Ar. Again we find much better agreement with correlated HF than uncorrelated HF. In particular comparison with the results of Perrot, aside from a difference in band gap, is in reasonable agreement considering the different treatments. It is also interesting to note the slight compression of the HF CB upon inclusion of correlation found by Perrot.
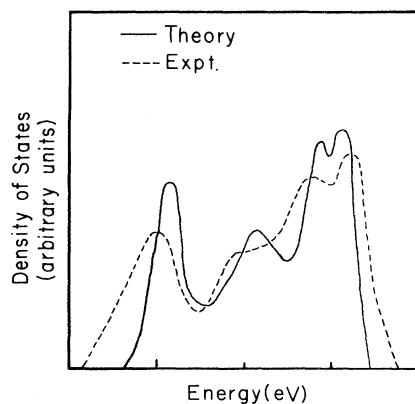

FIG. 6. DOS for the VB of the LiCl crystal (solid curve) and experimental photoelectron spectrum (dashed curve) of Ref. 45 with background baseline subtracted. Zero of the energy scale is arbitrary.

VII. DISCUSSION

The utility of a LDF approximation for electron exchange in the one-electron theory of insulators and semiconductors rests on its ability to produce an accurate and complete description of the electronic energy bands. The LDF theory has been very successful in treating ground-state properties, but in the past it has consistently underestimated the band gap by 30—40 % and produced an accurate description of only the valence region. This failure of the LDF approximation is attributed to the incomplete cancellation of the Coulomb self-interaction energy by the LDF self-exchange energy. The residual self-interaction has the effect of a nonuniform displacement of the occupied bands upward relative to the CB edge. This makes the LDF theory unsuitable for studying the numerous optical processes which require accurate wave functions and energies from the VB, CB, and core bands.

In this paper we have formulated a prescription for modifying the orthodox LDF theory of electronic energy bands from a fundamental standpoint to ensure complete cancellation of the self-interaction energy. We have also demonstrated its application to the LiCl and Ar crystals. In our formulation the first step is the construction of the self-interaction-free total-energy functional. Essential to our SIC formulation is the use of localized one-electron orbitals for evaluating the SIC terms in the energy functional. Upon expressing the energy functional in terms of the localized orbitals and applying the standard variation procedure, we derive the SIC Schrödinger equations for the localized orbitals. The atomiclike SIC potential for a localized orbital so derived bears much resemblance to the SIC potential for a free atom. However, for describing electronic processes in solid as well as for ease in solving the SCF equations, it is more convenient to express the one-electron orbitals in the Bloch form. For this purpose we utilize the linear relationship between the localized orbitals and the Bloch-state wave function and express the total energy exclusively in terms of the Bloch functions. Then we variationally derive the SCF Schrödinger equations for the Bloch-state wave functions. Each state-dependent Hamiltonian is found to contain a *periodic* SIC potential which at each lattice site consists of an atomiclike SIC potential multiplied by an amplitude weighting factor. The two sets of Schrödinger equations (for the localized orbitals and for the Bloch states) are, of course, equivalent. In actual calculations the Bloch form is more convenient. Furthermore the form of the *periodic* SIC potential mentioned above ensures that the Bloch-state solutions automatically reduce to the results of atomiclike states for energy bands with localized charge distribution. This provides a SIC potential which is applicable to both localized and extended states bridging the SIC for Bloch states with the atomiclike SIC potential for free atoms.

To facilitate solution of the SCF equations, a unified Hamiltonian is introduced to replace the individual state-dependent Hamiltonians. Based on a LCAO formulation, the matrix elements of the SIC potential are largely two-center integrals which can be computed easily. Inclusion of SIC in a LCAO framework involves only minor modification of the existing computer codes. Finally application of SIC-LSD to the LiCl and Ar crystals, in contrast

to the observed shortcomings of the LSD solution, generates a solution to the one-electron problem which achieves the stated goal of providing an accurate and complete description of the electronic energy bands, i.e., the band gap and core levels are in good agreement with experimental observations.

A unique feature of our formulation is the utilization of a local basis in construction of the total crystal energy. The breakdown of the LDF approximation occurs when condensation of the free-electron gas occurs. In a crystal, particularly an ionic crystal, the periodic crystal charge density deviates strongly from the free-electron behavior around every atom site. The choice of a local basis allows for the LDF approximation to be corrected when this breakdown occurs. The role of the localized orbitals can be viewed from the fundamental density-functional formalism. The energy functional in Eq. (1) consists of the non-SIC part $(T + V_{\mathrm{ext}} + U_C + E_{\mathrm{xc}})$ and the SIC term, U_{SIC}. Under an orbital transformation the non-SIC part (for full bands) remains invariant. The SIC energy per unit cell vanishes for the delocalized Bloch states. With localized orbitals the Coulomb part of U_{SIC} per unit cell is negative whereas the exchange part is positive. For the Ar crystal, the Coulomb and exchange parts of U_{SIC} per unit cell with the Wannier orbitals are -22.274 and 19.047 a.u., respectively. It is clear that localized orbitals, rather than Bloch functions, must be used in Eq. (4) for evaluating U_{SIC}. The preference of localized orbitals over the Bloch states for calculating E_t is a direct consequence of the SIC. In fact one should transform the Bloch functions into various sets of localized orbitals and the set which gives the most negative value for U_{SIC} would be the best choice. In the present paper we fix the choice of localized orbitals as the WF's. In the future it would be desirable to generate other sets of localized orbitals from the WF's (or the Bloch orbitals) to see if they may lead to even lower E_t.

Because of the complication involved in computing

WF's, in constructing the SIC potentials we introduce the approximation of replacing the Wannier charge density by the η functions and the WF's by the u functions (Sec. IV). In order to assess the effect of this approximation on the calculated energy-band structure let us consider a less sophisticated approximation in which we simply replace the WF's for the VB of LiCl by the free-atom $3p$ orbitals of Cl and the Wannier charge density by the free-atom orbital density. Application of this free-atom approximation to the SIC band calculation (without correlation) alters the band gap by 0.03 eV and the VB width by 0.04 eV as compared to the corresponding values listed in Table II. Thus the results are quite insensitive to the choice of the approximate version of the WF's as may be expected of insulators with localized charge distribution. For semiconductors the WF's differ very significantly from the atomic orbitals, hence accurate WF's are needed for SIC band calculations. Efforts to develop a simple, practical procedure for accurate determination of the WF's are underway.

Finally, we wish to restate the fact that in the calculations presented in Secs. V and VI we neglect the SIC potential for the CB states. Discussion of this point has been given in Sec. III C, but the question of SIC for the CB states is not fully answered. For large-gap insulators such as Ar and LiCl, the shift of the VB by the SIC is several eV; one can well expect the improvement in the energy-band gap to come mainly from the SIC shift of the VB. The SIC shift to the CB energies, however, may become much more important for semiconductors as a shift of CB by even a few tenths of an eV may significantly alter the band gap. Work is currently in progress to study the SIC of the CB states.

APPENDIX A

For a simple band the WF's satisfy Eq. (25). From the site orthogonality of the WF's we have

$$\epsilon_{n'\xi,nv} = \int w_{n'\sigma}^*(\vec{r} - \vec{R}_\xi) H_{n\sigma v} w_{n\sigma}(\vec{r} - \vec{R}_v) d\vec{r} \,. \tag{A1}$$

It follows from Eq. (25) that

$$\sum_v H_{n\sigma v} N^{-1/2} e^{i\vec{k}\cdot\vec{R}_v} w_{n\sigma}(\vec{r} - \vec{R}_v) = \sum_v N^{-1/2} e^{i\vec{k}\cdot\vec{R}_v} \sum_{n',\xi} \epsilon_{n'\xi,nv} w_{n'\sigma}(\vec{r} - \vec{R}_\xi) \,. \tag{A2}$$

With the use of Eq. (26) we convert the left-hand side (lhs) of Eq. (A2) into

$$\sum_v [H_0 + V_{n\sigma}^{\mathrm{SIC}}(\vec{r} - \vec{R}_v)] N^{-1/2} e^{i\vec{k}\cdot\vec{R}_v} w_{n\sigma}(\vec{r} - \vec{R}_v) = H_0 \psi_{n\sigma\vec{k}}(\vec{r}) + \sum_v N^{-1/2} e^{i\vec{k}\cdot\vec{R}_v} w_{n\sigma}(\vec{r} - \vec{R}_v) V_{n\sigma}^{\mathrm{SIC}}(\vec{r} - \vec{R}_v)$$

$$= H_{n\sigma\vec{k}} \psi_{n\sigma\vec{k}}(\vec{r}) \,, \tag{A3}$$

where $H_{n\sigma\vec{k}}$ is given by Eqs. (27)–(29). It is easily shown that $H_{n\sigma\vec{k}}$ is periodic in $\vec{R}_v$. The rhs of Eq. (A2) can be rewritten, by means of Eqs. (A1), (A3), and (26), as

$$\sum_{n',\xi} w_{n'\sigma}(\vec{r}-\vec{R}_\xi)\sum_\nu N^{-1/2}e^{i\vec{k}\cdot\vec{R}_\nu}\int w_{n'\sigma}^*(\vec{r}-\vec{R}_\xi)H_{n\sigma\nu}w_{n\sigma}(\vec{r}-\vec{R}_\nu)d\vec{r}$$

$$=\sum_{n',\xi} w_{n'\sigma}(\vec{r}-\vec{R}_\xi)\int w_{n'\sigma}^*(\vec{r}-\vec{R}_\xi)H_{n\sigma\vec{k}}\psi_{n\sigma\vec{k}}(\vec{r})d\vec{r}$$

$$=\sum_{n',\xi} w_{n'\sigma}(\vec{r}-\vec{R}_\xi)\int N^{-1/2}\sum_{\vec{k}'}e^{i\vec{k}'\cdot\vec{R}_\xi}\psi_{n'\sigma\vec{k}'}^*(\vec{r})H_{n\sigma\vec{k}}\psi_{n\sigma\vec{k}}d\vec{r}$$

$$=\sum_{n',\xi} w_{n'\sigma}(\vec{r}-\vec{R}_\xi)N^{-1/2}\sum_{\vec{k}'}e^{i\vec{k}'\cdot\vec{R}_\xi}\epsilon_{n'\vec{k},n\vec{k}}\delta_{\vec{k},\vec{k}'}$$

$$=\sum_{n',\xi} w_{n'\sigma}(\vec{r}-\vec{R}_\xi)N^{-1/2}e^{i\vec{k}\cdot\vec{R}_\xi}\epsilon_{n'\vec{k},n\vec{k}}=\sum_{n'}\epsilon_{n'\vec{k},n\vec{k}}\psi_{n'\sigma\vec{k}}(\vec{r}) \ . \quad \text{(A4)}$$

Combining this with Eqs. (A2) and (A3) we get

$$H_{n\sigma\vec{k}}\psi_{n\sigma\vec{k}}(\vec{r})=\sum_{n'}\epsilon_{n'\vec{k},n\vec{k}}\psi_{n'\sigma\vec{k}}(\vec{r}) \ .$$

APPENDIX B

The η local density is given by Eq. (55), and $u_{n\sigma\vec{k}}(\vec{r}-\vec{R}_\nu)$, defined in Eq. (53), is related to ψ as

$$\psi_{n\sigma\vec{k}}(\vec{r})=N^{-1/2}\sum_\nu e^{i\vec{k}\cdot\vec{R}_\nu}u_{n\sigma\vec{k}}(\vec{r}-\vec{R}_\nu) \ . \quad \text{(B1)}$$

The amount of charged enclosed by η is

$$\int \eta_{n\sigma}(\vec{r})d\vec{r}=N^{-1}\sum_{\vec{k},\xi}e^{i\vec{k}\cdot(\vec{R}_\nu-R_\xi)}$$

$$\times\int u_{n\sigma\vec{k}}^*(\vec{r}-\vec{R}_\xi)$$

$$\times u_{n\sigma\vec{k}}(\vec{r}-\vec{R}_\nu)d\vec{r}=1 \ . \quad \text{(B2)}$$

The $u_{n\sigma\vec{k}}$ functions are akin to the WF's because of the similarity of Eq. (B1) to Eq. (26). However, unlike the WF's, $u_{n\sigma\vec{k}}$ is $\vec{k}$ dependent and not site orthogonal. For a narrow-band crystal with small overlap between the atomic orbitals, the WF's can be well approximated by averaging $u_{n\sigma\vec{k}}(\vec{r}-\vec{R}_\nu)$ over k and imposing orthogonality to the first order, i.e.,

$$w_{n\sigma}(\vec{r})\simeq f_{n\sigma}(\vec{r})-\frac{1}{2}\sum_{\nu(\neq0)}(f_{n\sigma0}|f_{n\sigma\nu})f_{n\sigma}(\vec{r}-\vec{R}_\nu) \ , \quad \text{(B3)}$$

where

$$f_{n\sigma}(\vec{r})=AN^{-1}\sum_{\vec{k}}u_{n\sigma\vec{k}}(\vec{r}) \quad \text{(B4)}$$

and A is a normalization constant,

$$A^{-2}=\int \left| f_{n\sigma}(\vec{r})-\frac{1}{2}\sum_{\nu(\neq0)}(f_{n\sigma0}|f_{n\sigma\nu})f_{n\sigma}(\vec{r}-\vec{R}_\nu) \right|^2 d\vec{r} \ . \quad \text{(B5)}$$

Equating the rhs's of Eq. (26) and Eq. (B1), we utilize Eq. (B3) to group functions exclusively on the same site,

$$u_{n\sigma\vec{k}}(\vec{r})=\left[1-\frac{1}{2}\sum_{\nu(\neq0)}e^{-i\vec{k}\cdot\vec{R}_\nu}(f_{n\sigma0}|f_{n\sigma\nu})\right]f_{n\sigma}(\vec{r})$$

$$\simeq\left[1-\sum_{\nu(\neq0)}e^{-i\vec{k}\cdot\vec{R}_\nu}(f_{n\sigma0}|f_{n\sigma\nu})\right]^{1/2}f_{n\sigma}(\vec{r}) \ . \quad \text{(B6)}$$

Application of Eqs. (B1) and (B6) to Eq. (55) converts η into a summation over ν and $\vec{k}$ which, upon performing the $\vec{k}$ summation, reduces to

$$\eta_{n\sigma}(\vec{r})=[f_{n\sigma}(\vec{r})]^2-\sum_{\nu(\neq0)}(f_{n\sigma0}|f_{n\sigma\nu})f_{n\sigma}(\vec{r})f_{n\sigma}(\vec{r}-\vec{R}_\nu) \ . \quad \text{(B7)}$$

The Wannier charge density, according to Eq. (B3), is

$$|w_{n\sigma}(\vec{r})|^2\simeq|f_{n\sigma}(\vec{r})|^2$$

$$-\sum_{\nu(\neq0)}(f_{n\sigma0}|f_{n\sigma\nu})f_{n\sigma}(\vec{r})f_{n\sigma}(\vec{r}-\vec{R}_\nu)$$

$$+\cdots , \quad \text{(B8)}$$

where the ellipsis includes terms of the form $(f_{n\sigma0}|f_{n\sigma\nu})(f_{n\sigma0}|f_{n\sigma\xi})$. Hence in the case of small overlap $\eta(\vec{r})$ and $|w(\vec{r})|^2$ are equivalent.

APPENDIX C

If we approximate the Wannier charge density by the η local density, the SIC energy defined in Eq. (4) becomes

$$U_{\text{SIC}}=\sum_\nu U_{\text{SIC}}^\nu \ , \quad \text{(C1)}$$

$$U_{\text{SIC}}^\nu=-\sum_{n,\sigma}\{U_c[\eta_{n\sigma}(\vec{r}-\vec{R}_\nu)]+E_{\text{xc}}[\eta_{n\sigma}(\vec{r}-\vec{R}_\nu),0]\} \ . \quad \text{(C2)}$$

With the use of the new version of U_{SIC}, the SIC potential $\Delta V_{n\sigma\vec{k}}^{\text{SIC}}$ for each Bloch wave function $\psi_{n\sigma\vec{k}}$ is derived from part of a norm-conserving variation of the total energy E_t with respect to $\psi_{n\sigma\vec{k}}^*$ and is given by

$$\Delta V_{n\sigma\vec{k}}^{\text{SIC}}(\vec{r})=\frac{\sum_\nu\dfrac{\delta U_{\text{SIC}}^\nu}{\delta\eta_{n\sigma}(\vec{r}-\vec{R}_\nu)}\dfrac{\delta\eta_{n\sigma}(\vec{r}-\vec{R}_\nu)}{\delta\psi_{n\sigma\vec{k}}^*}}{\psi_{n\sigma\vec{k}}} \ . \quad \text{(C3)}$$

Performing the required variations yields Eqs. (57) and (56).

*Present address: Department of Physics, North Dakota State University, Fargo, ND 58105.

[1]J. C. Slater, *The Self-Consistent Field for Molecules and Solids* (McGraw-Hill, New York, 1974).

[2]P. Hohenberg and W. Kohn, Phys. Rev. 136, B864 (1964); W. Kohn and L. J. Sham, *ibid.* 140, A1133 (1965).

[3]R. D. Cowan, Phys. Rev. 163, 54 (1967).

[4]I. Lindgren, Int. J. Quantum Chem. Symp. 5, 411 (1971).

[5]J. P. Perdew, Chem. Phys. Lett. 64, 127 (1979).

[6]J. P. Perdew and A. Zunger, Phys. Rev. B 23, 5048 (1981).

[7]L. A. Cole and J. P. Perdew, Phys. Rev. A 25, 1265 (1982).

[8]J. P. Perdew and M. R. Norman, Phys. Rev. B 26, 5445 (1982).

[9]A. Zunger and A. J. Freeman, Phys. Rev. B 16, 2901 (1977).

[10]G. W. Bryant and G. D. Mahan, Phys. Rev. B 17, 1744 (1978).

[11]A. B. Kunz, R. S. Weidman, J. Boettger, and G. Cochran, Int. J. Quantum Chem. Symp. 14, 585 (1980).

[12]R. A. Heaton and C. C. Lin, Phys. Rev. B 22, 3629 (1980).

[13]A. Zunger and M. L. Cohen, Phys. Rev. B 18, 5449 (1978).

[14]R. A. Heaton, J. G. Harrison, and C. C. Lin, Solid State Commun. 41, 827 (1982).

[15]See, for example, J. E. Lennard-Jones and J. A. Pople, Proc. R. Soc. London Ser. A 202, 166 (1950); K. Ruedenberg, in *Computational Methods for Large Molecules and Localized States in Solids*, edited by F. Herman, A. D. McLean, and R. K. Nesbet (Plenum, New York, 1973).

[16]W. Kohn, Phys. Rev. B 7, 4388 (1973).

[17]J. des Cloizeaux, Phys. Rev. 129, 554 (1963); J. von Boehm and J.-L. Calais, J. Phys. C 12, 3661 (1979).

[18]See, for example, N. F. Mott and R. W. Gurney, *Electronic Processes in Ionic Crystals* (Dover, New York, 1964); R. S. Knox and K. J. Teegarden, in *Physics of Color Centers*, edited by W. B. Fowler (Academic, New York, 1968), Chap. 1.

[19]G. H. Wannier, Phys. Rev. 52, 191 (1937); J. C. Slater, Adv. Quantum Chem. 6, 1 (1972); MIT Solid State and Molecular Theory Group Semi-Annual Report No. 71, July 1969 (unpublished).

[20]See, for example, S. Doniach, in *Computational Methods in Band Theory*, edited by P. M. Marcus, J. F. Janak, and A. R. Williams (Plenum, New York, 1971), p. 500.

[21]See, for example, A. C. Hurley, *Introduction to the Electron Theory of Small Molecules* (Academic, New York, 1976).

[22]J. G. Harrison, R. A. Heaton, and C. C. Lin, J. Phys. B 16, 2079 (1983).

[23]A. Veillard, Theor. Chim. Acta 12, 405 (1968).

[24]R. C. Chaney, E. E. Lafon, and C. C. Lin, Phys. Rev. B 4, 2734 (1971).

[25]R. Haensel, G. Keitel, E. E. Koch, M. Skibowski, and P. Schreiber, Phys. Rev. Lett. 23, 1160 (1969).

[26]N. Schwentner, F.-J. Himpsel, V. Saile, M. Skibowski, W. Steinmann, and E. E. Koch, Phys. Rev. Lett. 34, 528 (1975).

[27]R. Haensel, G. Keitel, N. Kosuch, U. Nielsen, and P. Schreiber, J. Phys. (Paris) Colloq. 32, C4-236 (1971).

[28]J. A. Bearden and A. F. Burr, Rev. Mod. Phys. 39, 125 (1967).

[29]U. Rössler, in *Rare Gas Solids,* edited by M. L. Klein and J. A. Venables (Academic, New York, 1976), Vol. I.

[30]M. Alterelli, W. Andreoni, and F. Bassani, Solid State Commun. 16, 143 (1975).

[31]N. O. Lipari and W. B. Fowler, Phys. Rev. B 2, 3354 (1970).

[32]N. O. Lipari, Phys. Rev. B 6, 4071 (1972).

[33]L. Dagens and F. Perrot, Phys. Rev. B 5, 641 (1972).

[34]A. B. Kunz and D. J. Mickish, Phys. Rev. B 8, 779 (1973).

[35]S. Baroni, G. Grosso, and G. Pastori Parravicini, Phys. Rev. B 23, 6441 (1981).

[36]J. E. Robinson, F. Bassani, R. S. Knox, and J. R. Schrieffer, Phys. Rev. Lett. 9, 215 (1962).

[37]Figure 3 of Ref. 11 is described as the results of Ar. However, it is apparent that Fig. 2 corresponds more closely to the results of Ar. We thank Professor A. B. Kunz for helpful conversation.

[38]U. von Barth and L. Hedin, J. Phys. C 5, 1629 (1972).

[39]E. P. Wigner, Phys. Rev. 46, 1002 (1934); N. D. Lang and W. Kohn, Phys. Rev. B 1, 4555 (1970); O. Gunnarsson and B. I. Lundqvist, *ibid.* 13, 4274 (1976); D. M. Ceperley, *ibid.* 18, 3126 (1978); D. M. Ceperley and B. J. Alder, Phys. Rev. Lett. 45, 566 (1980); G. S. Painter, Phys. Rev. B 24, 4264 (1981).

[40]J. G. Harrison and C. C. Lin, Phys. Rev. B 23, 3894 (1981).

[41]R. C. Chaney, T. K. Tung, C. C. Lin, and E. E. Lafon, J. Chem. Phys. 52, 361 (1970).

[42]K. Teegarden and G. Baldini, Phys. Rev. 155, 896 (1967).

[43]G. Baldini and B. Bossachi, Phys. Status Solidi 38, 325 (1970).

[44]S. T. Pantelides and F. C. Brown, Phys. Rev. Lett. 33, 298 (1974).

[45]R. T. Poole, J. G. Jenkins, R. C. G. Leckey, and J. Liesegang, Chem. Phys. Lett. 22, 101 (1973).

[46]S. T. Pantelides, Phys. Rev. B 11, 2391 (1975).

[47]T. Ohta, S. Kinoshita, and H. Kuroda, J. Electron Spectrosc. Relat. Phenom. 12, 169 (1977).

[48]H. Saito, S. Saito, and R. Onaka, J. Phys. Soc. Jpn. 27, 126 (1969).

[49]R. Haensel, C. Kunz, and B. Sonntag, Phys. Rev. Lett. 20, 262 (1968).

[50]P. H. Citrin and T. D. Thomas, J. Chem. Phys. 57, 4446 (1972).

[51]In Ref. 46, Pantelides obtained the Li 1s core level by utilizing the data of Citrin and Thomas (Ref. 50). Since the authors of Ref. 50 regard their XPS LiCl data as unreliable, we reanalyze the Li 1s level using the soft-x-ray spectra of Ref. 49. This places the Li 1s band 51.7±1.0 eV below the VB centroid, as compared to 51.5 eV based on Pantelides's result.

[52]A. B. Kunz, Phys. Rev. B 2, 5015 (1970).

[53]A. B. Kunz, Phys. Rev. B 12, 5890 (1975).

[54]A. B. Kunz, Phys. Rev. B 26, 2056 (1982).

[55]F. Perot, Phys. Status Solidi B 52, 163 (1972).